Behavior of horizontally curved reinforced concrete beam-and-slab bridges

Tarek I. Ebeido
Structural Eng. Dept., Faculty of Eng., Alexandria University, Alexandria, Egypt

In this paper, an experimental-theoretical investigation was conducted in order to study the behavior of horizontally curved reinforced concrete beam-and-slab bridges over the complete range of loading up to the bridge failure. The experimental program conducted in this paper included the fabrication, instrumentation, and testing of two reinforced concrete beam-and-slab bridge models. One of these bridge models was rectangular in plan whereas the other bridge model was horizontally curved. Thus the effect of curvature was extensively investigated when comparing the results of testing the two bridge models. The effect of curvature was investigated from the point of view of the following: (i) vertical deflections of longitudinal girders; (ii) steel strains; (iii) support reactions; (iv) cracking loads; (v) failure loads; (vi) cracking patterns; and (vii) failure modes. It was found that the effect of curvature on the behavior of reinforced concrete beam-and-slab bridges is extremely significant both in the elastic range of loading and also in the post-elastic range of loading up to failure. It was found also that the redistribution phenomena took place much more significantly in the case of curved bridge model than that in the case of straight rectangular bridge model. Furthermore, a finite element model was developed. The reliability of the model was confirmed using the current experimental results. The finite element model was then employed to conduct a detailed parametric study on prototype horizontally curved reinforced concrete beam-and-slab bridges. The effect of all major parameters on the support reactions was investigated. Finally the results of the parametric study was used to develop a simple empirical method for the calculation of support reactions in horizontally curved reinforced concrete beam-and-slab bridges utilizing the standard truck specified in the Egyptian code for calculation of loads and forces in structures and buildings.

فى هذا البحث، تم عمل دراسة معملية - نظرية لدراسة سلوك الكبارى الخرسانية المسلحة المنحنية المكونة من كمرات وبلاطات وذلك خلال مرحلة المرونة وكذلك فى مرحلة مابعد التشريخ وحتى الإنهيار. تضمن البرنامج المعملى صب وتجهيز وإختبار نموذجين لكبارى خرسانية مسلحة مكونة من بلاطات وكمرات. أحد هذين النموذجين كان على شكل مستطيل فى المسقط الأفقى بينما كان النموذج الأخر منحنى فى المسقط الأفقى. بذلك تم دراسة تأثير الإنحناء فى المسقط الأفقى عن طريق مقارنة نتائج إختبار النموذجين. تم دراسة تأثير الإنحناء من النواحى التالية: ١ سهم الإنحناء الرأسى للكمرات؛ ٢ الإنفعال فى حديد التسليح؛ ٣ ردود الأفعال ؛ ٤ حمل التشريح ؛ ٥ حمل الإنهيار ؛ ٦ شكل التشريح ؛ ٧ شكل الإنهيار. وقد وجد أن الإنحناء فى المسقط الأفقى يؤثر تأثيراً كبيراً على سلوك الكبارى الخرسانية المسلحة المكونة من بلاطات وكمرات وذلك فى مرحلة المرونة وكذلك فى مرحلة مابعد التشريح وحتى الإنهيار. وقد كان لظاهرة إعادة التوزيع أثراً أكبر فى حالة نموذج الكوبرى المنحنى فى المسقط الأفقى عن تلك فى حالة نموذج الكوبرى المستطيل.بالإضافة إلى ذلك تم عمل نموذج نظرى بإستخدام طريقة العناصر المحددة. وقد تم التأكد من صلاحية النموذج النظرى بمقارنة النتائج النظرية بالنتائج المعملية. تم إستخدام النموذج النظرى فى عمل دراسة بارامترية على كبارى خرسانية مسلحة منحنية فى المسقط الأفقى مكونة من كمرات وبلاطات بأبعاد حقيقية. وقد تم دراسة تأثير جميع العوامل الرئيسية على ردود أفعال الكبارى. أخيراً تم إستخدام نتائج الدراسة البارامترية فى التوصل إلى طريقة بسيطة لحساب ردود أفعال الكبارى الخرسانية المسلحة المنحنية فى المسقط الأفقى المكونة من بلاطات وكمرات تحت تأثير أحمال عربات النقل الثقيل القياسية المنصوص عليها فى الكود المصرى لحساب الأحمال والقوى فى الأعمال الإنشائية وأعمال المبانى.

Keywords: Beam, Bridges, Curved, Load distribution, Reinforced concrete

1. Introduction

During the first half of the nineteenth century, Saint-Venant published a memoir that marked the birth of all research efforts published to date on the analysis and design of horizontally curved girders. The employment of horizontally curved beam-and-slab bridges in elevated highways has remarkably increased during the last few decades. This is due to the frequent demand for these geometries in modern highway networks.

However, most of the investigations found in the literature regarding the behavior of reinforced concrete beam-and-slab bridges have been directed towards rectangular straight bridges. Comparatively, very little research efforts have considered the behavior of horizontally curved reinforced concrete beam-and-slab bridges.

1.1. Behavior of straight rectangular beam-and-slab bridges

Many researchers have investigated the behavior of straight rectangular reinforced concrete beam-and-slab bridges [1 to 8]. Furthermore, a detailed study [9] presented a comparison of the behavior of simple and continuous bridges under the effect of truck loads given in different codes of practice. The knowledge of actual girder distribution factors is extremely important for a rational design and evaluation of bridges. Many investigations found in the literature have studied load distribution in straight rectangular beam-and-slab bridges. However, through all these investigations the truck specified by the American Association of State Highway and Transportation Officials AASHTO [10] was considered. Tarhini and Frederick [11] presented new lateral load distribution formula for bending moment in beam-and-slab bridges, based on a finite element analysis. Results of field tests on beam-and-slab bridges [12] indicated that measured girder distribution factors are consistently lower than those of the AASHTO methods. Several other studies found in the literature have considered load distribution in beam-and-slab bridges [13 to 17]. Several methods of analysis were found in the literature for beam-and-slab bridges. Analytical models for the non linear analysis of reinforced concrete beam-and-slab bridges were developed utilizing the finite element method [18 and 19]. Load and resistance models were developed for the design of new bridges and the evaluation of existing ones [20]. Furthermore, finite element failure analysis of reinforced concrete T-girder bridges was presented [21].

1.2. Behavior of curved beam-and-slab bridges

As the population of Egypt grows, there will be a need for smooth traffic flow in highways and major roadways. This will require curved roadway alignment, and will often require curved bridges. In early days of curved bridge design and construction, bridge superstructures supporting curved roadway alignment were comprised of short straight girders linked together at the supports [22]. As the technology for designing curved bridges became available, it became possible to design curved bridges. However, due to the simple addition of curvature, the design of bridges becomes extremely more complicated than that of straight rectangular bridges. Girders of straight rectangular bridges can be designed by isolating each member and applying standard trucks. However, very little research efforts have been directed towards the study of the behavior of horizontally curved reinforced concrete beam-and-slab bridges. The behavior of reinforced concrete curved bridges was extensively investigated [23 and 24]. However, the type of structure considered was the waffle slab structure. Another investigation [25] has considered the nonlinear elastic behavior of horizontally curved girders that have significant actions perpendicular to their planes. Recently, another study [26] has investigated live load moment distribution for horizontally curved beam-and-slab bridges. New approximate moment distribution factor equations were presented. Such equations are useful in combination with the truck specified by the AASHTO code [10].

1.3. The required research

From the above presented literature review it is observed that most of the investigations found regarding the behavior of reinforced concrete beam-and-slab bridges have been directed towards rectangular straight bridges. Comparatively, very little research efforts have considered the behavior of horizontally curved reinforced concrete beam-and-slab bridges. None of the previous investigations found in the literature has considered the behavior of horizontally curved reinforced concrete beam-

and-slab bridges in the post elastic range of loading up to failure. None of the previous investigations found in the literature has considered the distribution of reactions in horizontally curved reinforced concrete beam-and-slab bridges over the complete range of loading up to failure. Furthermore, although the analysis of curved bridges is much more complex than that of straight bridges, there are no methods for the determination of support reactions in curved bridges integrated into different codes of practice such as the AASHTO code [10]. There is however the "Guide Specifications for Horizontally Curved Highway Bridges" [27]. This guide is widely recognized to be outdated, disjointed, and difficult to use [22]. Moreover, although the Egyptian Code for Calculation of Loads and Forces in Structures and Buildings [28] specifies the use of a specific standard truck presented in the code. However, no equations are presented in any Egyptian code for the calculation of support reactions in horizontally curved reinforced concrete beam-and-slab bridges. Therefore, it is important to develop a simple method for the calculation of support reactions in horizontally curved reinforced concrete beam-and-slab bridges utilizing the standard truck specified in the Egyptian Code for Calculation of Loads and Forces in Structures and Buildings [28].

1.4. The current research

This paper presents results from an experimental-theoretical investigation on the behavior of horizontally curved reinforced concrete beam-and-slab bridges over the complete range of loading up to the bridge failure. The experimental program conducted in this paper included the fabrication, instrumentation, and testing of two reinforced concrete beam-and-slab bridge models. One of these bridge models was rectangular in plan whereas the other bridge model was horizontally curved. Thus the effect of curvature was extensively investigated when comparing the results of testing the two bridge models. The effect of curvature was investigated from the point of view of the following: (i) vertical deflections of girders; (ii) steel strains; (iii) support reactions; (iv) cracking loads; (v) failure loads; (vi) cracking patterns; and (vii) failure modes. The effect of curvature was investigated both in the elastic range of loading and also in the post-elastic range of loading up to failure. A finite element model was developed. The reliability of the model was confirmed using the current experimental results. The finite element model was then employed to conduct a detailed parametric study on prototype horizontally curved reinforced concrete beam-and-slab bridges. The effect of all major parameters on the support reactions was investigated. Finally the results of the parametric study was used to develop a simple empirical method for the calculation of support reactions in horizontally curved reinforced concrete beam-and-slab bridges utilizing the standard truck specified in the Egyptian Code for Calculation of Loads and Forces in Structures and Buildings [28].

2. Experimental program

The experimental program conducted in this paper included casting, instrumentation, and testing two reinforced concrete beam and slab bridge models. One of these bridge models was rectangular in plan whereas the other bridge model was horizontally curved. The main objectives of the experimental program were: (i) to investigate the effect of curvature on the behavior of reinforced concrete beam and slab bridges over the complete range of loading up to the failure of the bridge; and (ii) to confirm the results of the theoretical model developed in this paper for the analysis of reinforced concrete beam and slab bridges.

Dimensions and reinforcement details for tested bridge models are presented in figs. 1 and 2. The first bridge model was rectangular in plan having a total length of 3500 mm and a span length of 3400 mm, whereas the second bridge model was horizontally curved. The total length of the curved bridge model was 3500 mm measured at the mid-width of the bridge model. The span length of the curved bridge model was 3400 mm measured at the mid-width of the bridge model. The radius of curvature of the bridge model was 5000 mm at mid-width. The central angle was 40 degrees. Each of the tested bridge models

was provided by three longitudinal girders having a width of 100 mm and a depth of 200 mm. Both tested bridge models were provided with end diaphragms having a width of 100 mm and a depth of 200 mm. The reinforcement of the longitudinal girders and end diaphragms consisted of two bars diameter 12 mm high tensile steel longitudinal bottom reinforcement, two bars diameter 10 mm high tensile steel longitudinal top reinforcement, and transverse stirrups consisting of five bars per meter diameter 6 mm mild steel. For both tested bridge models the slab thickness was 50 mm. The slabs were provided by two layers of reinforcement. For the straight rectangular bridge model each layer consisted of five bars per meter diameter 6 mm mild steel in the longitudinal direction and five bars per meter diameter 6 mm mild steel in the transverse direction. For the curved bridge model each layer consisted of five bars per meter diameter 6 mm mild steel in the radial direction measured at the mid width of the bridge model, and tangential reinforcement comprising five bars per meter diameter 6 mm mild steel.

The yield strength and ultimate strength of the steel reinforcement used were 245 MPa and 370 MPa, respectively for mild steel diameter 6 mm. and were 424 MPa and 595 MPa, respectively for high tensile steel diameter 12 mm. The concrete mix used for tested bridge models was made using locally produced commercially available ordinary Portland cement type I, locally available natural desert sand, and broken stones having a maximum size of 10 mm. The mix proportions were 1.0: 1.6: 2.55, respectively by weight. The water cement ratio w/c was kept in the range of 0.4. Control specimens of 150 mm cubes were made from each concrete batch and the average 28-day concrete cube compressive strength f_{cu} was 36 MPa. Bridge models were tested to failure under the effect of eccentric load applied at the mid span of each bridge model as shown in figs. 1 and 2. The load was applied to the bridge models using a hydraulic jack of 500 kN capacity. The applied load was monitored by means of a load cell. The load was applied in increments of 5 kN until the failure of each bridge model.

Deflections of longitudinal girders of the bridge models were measured at mid span of each girder by means of three mechanical dial gauges with a travel sensitivity of 0.01 mm. The locations of these dial gauges are shown in fig. 2. Strains in longitudinal bottom tension reinforcement of the longitudinal girders at mid span were measured using electrical resistance strain gauges with 10 mm gauge length. For each tested bridge model strain gauges were attached to one of the bottom longitudinal bars of the three girders at mid span. Furthermore, support reactions were monitored by means of six load cells each having a capacity of 100 kN as shown in fig. 2. Fig. 3 shows loading setup for tested bridge models.

3. Experimental results and discussions

Two reinforced concrete beam and slab bridge models were tested to failure within the current experimental program. One of these bridge models was rectangular in plan whereas the other bridge model was horizontally curved. The main objective of the experimental program was to investigate the effects of bridge curvature on the behavior of reinforced concrete beam and slab bridges over the complete range of loading up to failure. Such effects shall be discussed in the following sections and shall include: (i) mid-span deflections of longitudinal girders; (ii) steel strains; (iii) support reactions; (iv) cracking loads and failure loads; and (v) cracking patterns and failure modes. The effects of curvature shall be assessed when comparing the experimental results obtained from testing the rectangular straight bridge model to those obtained from testing the curved bridge model.

The experimental results for both reinforced concrete bridge models are summarized in table 1. The experimental results included cracking loads and failure loads. Table 1 also lists mid-span deflections and support reactions for the three longitudinal girders within the elastic range of loading at a load 10 kN as an example. Moreover, the table lists mid-span deflections and support reactions for the three longitudinal girders at failure. Fig. 4 shows

Fig. 1. Dimensions and reinforcement details for tested bridge models.

Fig. 2. Loading setup and instrumentation for tested bridge models.

(a) Straight bridge model

(b) Curved bridge model

Fig. 3. Tested bridge models under load.

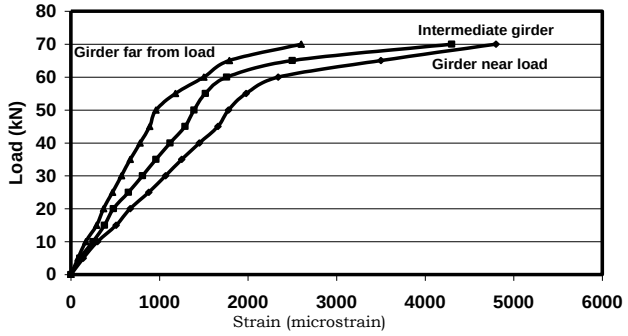

(a) Straight bridge model

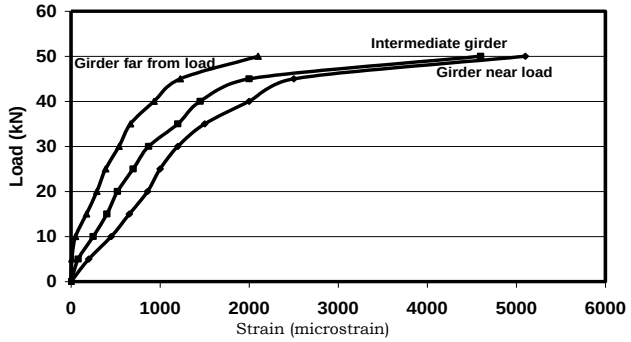

(b) Curved bridge model

Fig. 4. Load-strain relationships for tested bridge models.

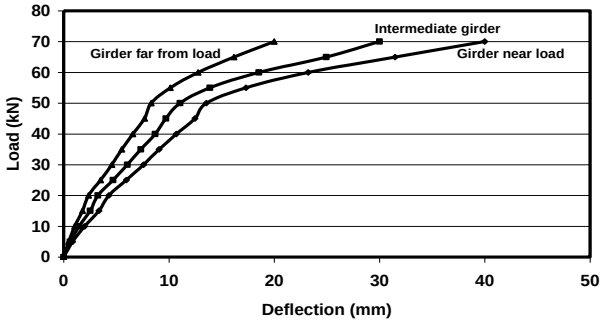

(a) Straight bridge model

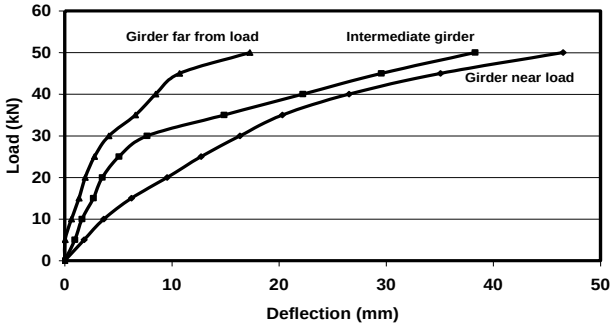

(b) Curved bridge model

Fig. 5. Load-deflection relationships for tested bridge models.

load-strain relationships for both tested straight and curved bridge models. Fig. 5 shows load-deflection relationships for tested bridge models. Fig. 6 shows load-support reaction relationships for tested bridge models. Figs. 7, 8, and 9 show the effects of curvature on longitudinal steel strains, mid-span deflections, and support reactions, respectively. It should be noted that these effects are presented for the girder near load, the intermediate girder, and the girder far from load. Fig. 10 shows failure modes for tested straight and curved bridge models.

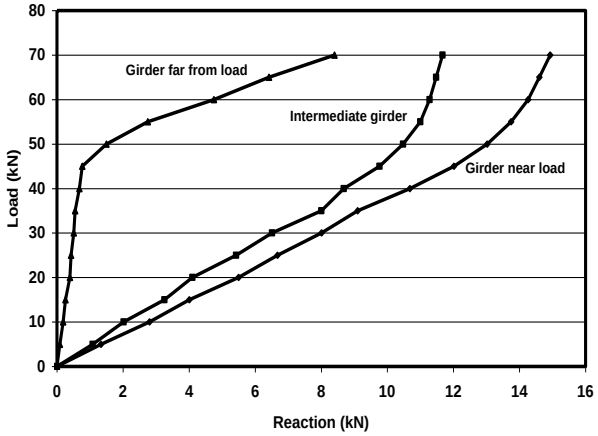

(a) Straight bridge model

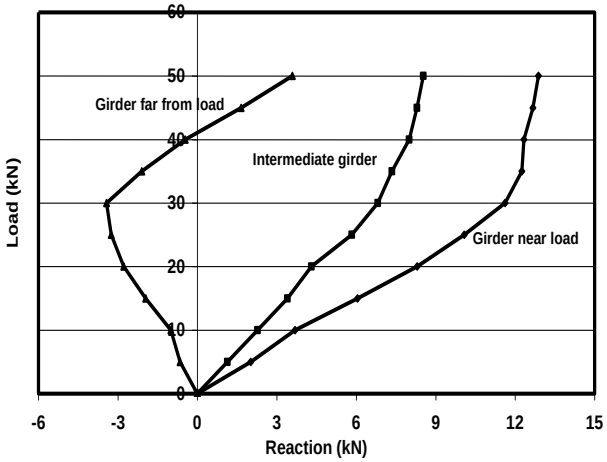

(b) Curved bridge model

Fig. 6. Load-reaction relationships for tested bridge models.

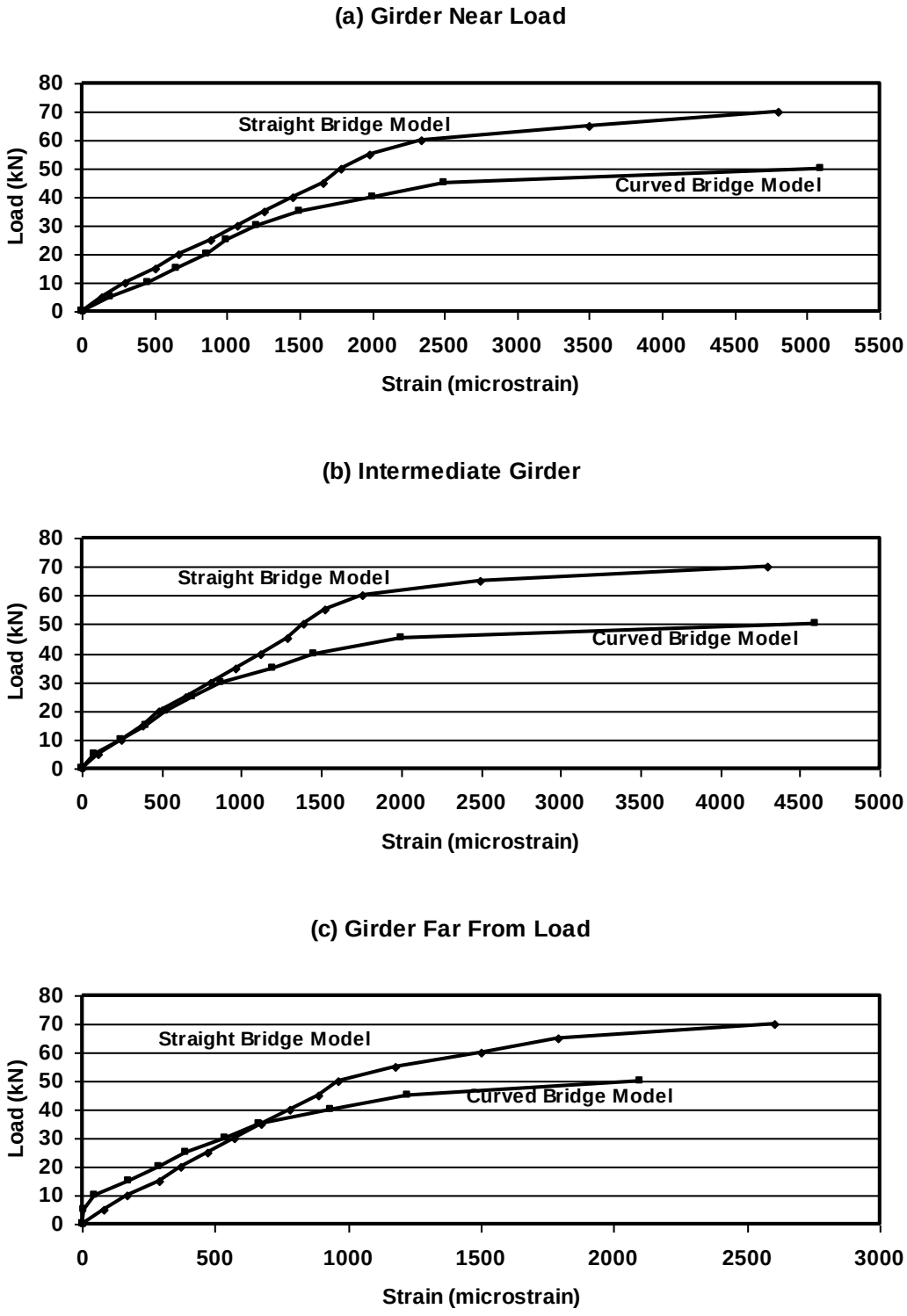

Fig. 7. Effect of curvature on steel strains for tested bridge models.

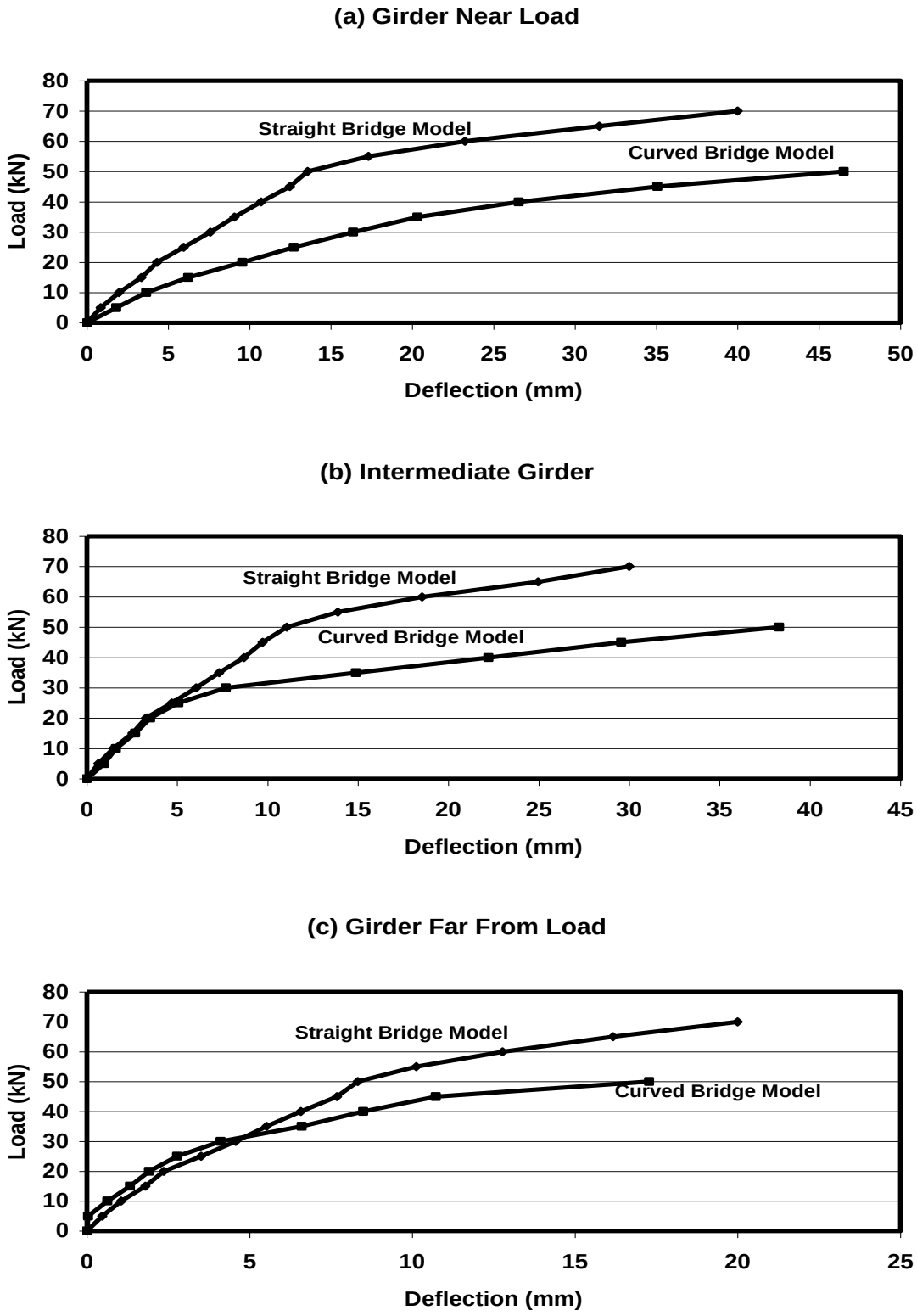

Fig. 8. Effect of curvature on deflections for tested bridge models.

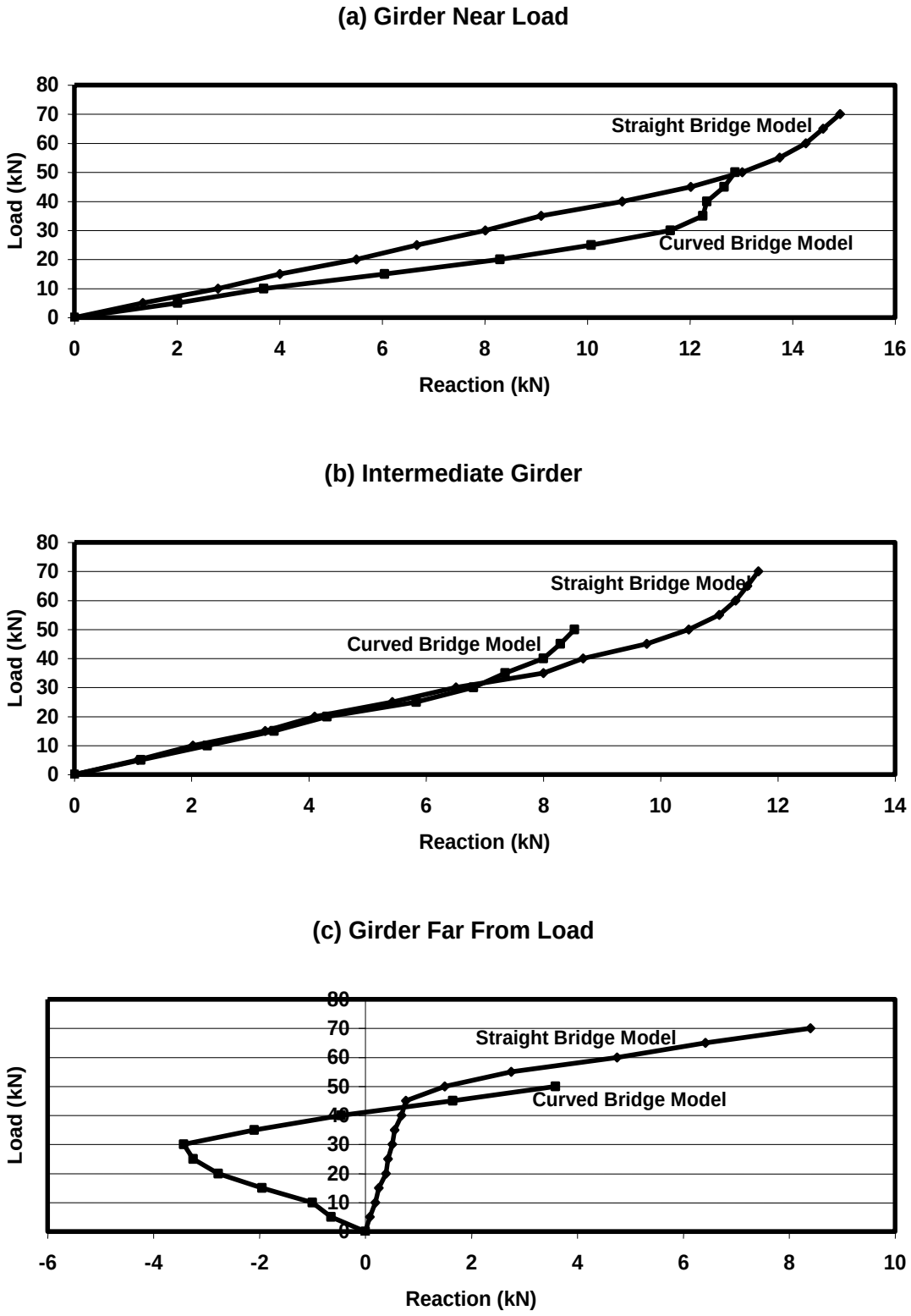

Fig. 9. Effect of curvature on support reactions for tested bridge models.

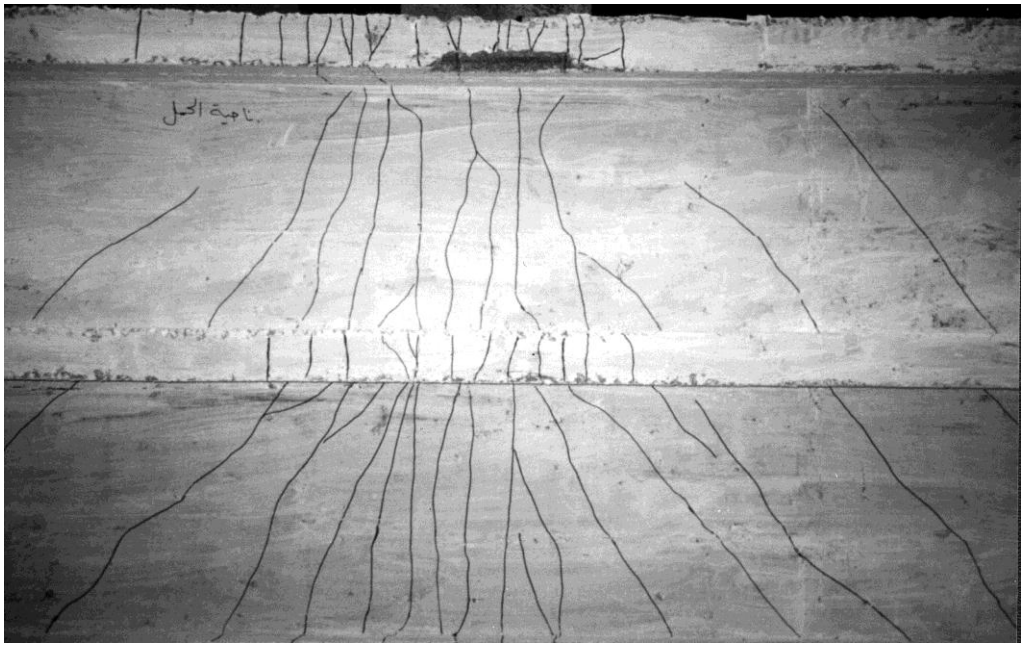

(a) Straight bridge model

(b) Curved bridge model

Fig. 10. Cracking patterns for tested bridge models.

3.1. Deflections

It can be observed that bridge curvature significantly influenced mid-span deflections of all bridge models girders not only within the elastic range of loading but also in the post-elastic range of loading up to failure of the bridge models as shown in fig. 8. The values of deflections within the elastic range at a load 10 kN are listed in table 1, for both straight and curved bridge models. For the straight bridge model the value of such elastic deflection was 1.98 mm, 1.46 mm, and 1.05 mm, respectively for the girder near load, the intermediate girder, and the girder far from load. It should be noted that the significant variation in the values of mid-span deflection from girder to another was due to the fact that the load was eccentrically applied to the bridge model. The deflection of the girder far from load was about 53% of that of the girder near load. The values of mid-span deflection for the straight bridge model at failure were 41.11 mm, 29.35 mm, and 19.25 mm, respectively for the girder near load, the intermediate girder, and the girder far from load. The deflection of the girder far from load at failure was about 47% of that of the girder near load.

In the case of curved bridge model the values of the deflection within the elastic range at load 10 kN were 3.65 mm, 1.61 mm, and 0.63 mm, respectively for the girder near load, the intermediate girder, and the girder far from load. Comparing the results of the deflection within the elastic range for the straight bridge model to those for the curved bridge model, the effect of curvature may be summarized as follows: (i) for the girder near load the deflection increased from 1.98 mm for the straight bridge model to 3.65 mm for the curved bridge model, representing about 84% increase as a result of curvature; (ii) for the intermediate girder the deflection increased from 1.46 mm for the straight bridge model to 1.61 mm for the curved bridge model, representing about 10% increase as a result of curvature; and (iii) for the girder far from load the deflection decreased from 1.05 mm for the straight bridge model to 0.63 mm for the curved bridge model, representing about 40% decrease as a result of curvature.

From the above presented results it can be concluded that bridge curvature significantly influences the deflection of the longitudinal girders of beam and slab bridges within the elastic range of loading in the following manner: (i) significant increase in the deflection of the outer longer girder; and (ii) significant decrease in the deflection of the inner shorter girder. It should be noted that bridge curvature continued to influence longitudinal girders deflection in the post-elastic range of loading up to failure as shown in fig. 8. However, it can be observed that at any given load within the post-elastic range of loading curvature resulted in a significant increase in the mid-span deflection of all longitudinal girders of the bridge models, including the inner shorter girder far from load.

At failure the values of mid-span deflection for the curved bridge model were 46.52 mm, 38.29 mm, and 17.28 mm, respectively for the girder near load, the intermediate girder, and the girder far from load. Comparing the results of the deflection at failure for the straight bridge model to those for the curved bridge model, the effect of curvature may be summarized as follows: (i) for the girder near load the deflection increased from 41.11 mm for the straight bridge model to 46.52 mm for the curved bridge model, representing about 13% increase as a result of curvature; (ii) for the intermediate girder the deflection increased from 29.35 mm for the straight bridge model to 38.29 mm for the curved bridge model, representing about 30% increase as a result of curvature; and (iii) for the girder far from load the deflection decreased from 19.25 mm for the straight bridge model to 17.28 mm for the curved bridge model, representing about 10% decrease as a result of curvature.

From the above presented results it can be concluded that bridge curvature influences the deflection of the longitudinal girders of beam and slab bridges at failure in the following manner: (i) increase in the deflection of the outer longer girder; (ii) increase in the deflection of the intermediate girder; and (iii) decrease in the deflection of the inner shorter girder. It should be noted that the effect of curvature on the deflection of the longitudinal

girders was much more significant within the elastic range of loading than that at failure. Such variation in the effect of curvature may be attributed to the fact that in the case of curved bridges redistribution phenomena have significantly took place at failure leading to a more uniform distribution of deflections between longitudinal girders. For example, in the elastic range of loading, the ratio between the deflection of the inner shorter girder far from load to that of the outer longer girder near load was about 1:5.8. However, such ratio decreased at failure to only 1:2.7.

3.2. Longitudinal steel strains

Examining figs 4 and 7, the significant influence of bridge curvature on longitudinal steel strains can be observed. Such influence can be detected within the elastic range of loading and also within the post-elastic range of loading up to failure of bridge models. The values of longitudinal steel strains within the elastic range at a load 10 kN for the straight bridge model were 300, 250, and 170 microstrain, respectively for the girder near load, the intermediate girder, and the girder far from load. It can be observed that the longitudinal steel strain for the girder far from load is about 57% of that for the girder near load. Such significant variation in the values of longitudinal steel strain from a girder to another is attributed to the fact that the load was eccentrically applied to the bridge model.

The longitudinal steel reinforcement of the girder near load yielded at a load representing about 79% of the bridge failure load whereas that of the intermediate girder yielded at a load representing about 89% of the bridge failure load. The longitudinal steel reinforcement of the girder far from load yielded at the bridge failure load. It should be noted that at the bridge failure load the values of the strains in the longitudinal steel reinforcement exceeded the ultimate steel strain for both the girder near load and the intermediate girder. Also, at failure the longitudinal steel strain for the girder far from load was about 51% of that for the girder near load.

The values of longitudinal steel strain within the elastic range at a load 10 kN for the curved bridge model were 450, 249, and 50 microstrain, respectively for the girder near load, the intermediate girder, and the girder far from load. A comparison between the values of longitudinal steel strain within the elastic range of loading for the straight bridge model to those for the curved bridge model, one can observe the following: (i) the longitudinal steel strain increased from 300 microstrain for the straight bridge model to 450 microstrain for the curved bridge model, for the girder near load, representing about 50% increase as a result of curvature; (ii) the longitudinal steel strain for the intermediate girder was not affected by curvature; and (iii) the longitudinal steel strain decreased from 170 microstrain for the straight bridge model to 50 microstrain for the curved bridge model, for the girder far from load, representing about 71% decrease as a result of curvature. Therefore, it can be concluded that bridge curvature significantly affects the longitudinal steel strain of reinforced concrete beam and slab bridges within the elastic range of loading. Such effects can be summarized as follows: (i) significant increase in the longitudinal steel strain for the outer longer girder; and (ii) significant decrease in the longitudinal steel strain for the inner shorter girder.

Furthermore, bridge curvature continued to influence longitudinal steel strain in the post-elastic range of loading up to failure as shown in fig. 7. It should be noted that bridge curvature resulted in a significant increase in the longitudinal steel strain within the post-elastic range of loading. This was observed at any given load within the post-elastic range of loading and for all longitudinal girders of the bridge models even for the inner shorter girder far from load.

In the case of curved bridge model, the longitudinal steel reinforcement of the girder near load yielded at a load representing about 85% of the bridge failure load whereas that of the intermediate girder yielded at a load representing about 93% of the bridge failure load. However, the longitudinal steel reinforcement of the girder far from load yielded at the bridge failure load. Also, at bridge failure load the values of the strain in the longitudinal steel reinforcement exceeded

the ultimate steel strain for both the girder near load and the intermediate girder. Comparing the results of longitudinal steel strain at failure for the straight bridge model to those for the curved bridge model, the effect of curvature may be summarized as follows: (i) the longitudinal steel strain increased from 4800 microstrain for the straight bridge model to 5100 microstrain for the curved bridge model, for the girder near load, representing about 6% increase as a result of curvature; (ii) the longitudinal steel strain increased from 4300 microstrain for the straight bridge model to 4600 microstrain for the curved bridge model, for the intermediate girder, representing about 7% increase as a result of curvature; and (iii) the longitudinal steel strain decreased from 2600 microstrain for the straight bridge model to 2100 microstrain for the curved bridge model, for the girder far from load, representing about 19% decrease as a result of curvature.

Therefore, it can be concluded that the bridge curvature affects the longitudinal steel strain for the longitudinal girders of reinforced concrete beam and slab bridges. Such effects can be summarized as follows: (i) increase in the longitudinal steel strain for the outer longer girder; (ii) increase in the longitudinal steel strain for the intermediate girder; and (iii) decrease in the longitudinal steel strain for the inner shorter girder. It was also observed that the effect of curvature on the longitudinal steel strain was much more significant in the elastic range of loading than that at failure. As mentioned before, such variation in the effect of curvature may be attributed to the fact that in the case of curved bridges redistribution phenomena have significantly took place at failure leading to a more uniform distribution of loads between longitudinal girders. For example, within the elastic range at load 10 kN, the ratio between the longitudinal steel strain of the inner shorter girder far from load to that of the outer longer girder near load was about 1:9. However, such ratio dropped to only 1:2.4 at failure.

3.3. Support reactions

As mentioned before, very limited research efforts were directed towards the study of the effect of bridge curvature on the distribution of support reactions in reinforced concrete beam and slab bridges, although it was found herein that such curvature has a great influence on the support reaction distribution. This effect can be clearly detected when examining figs 6 and 9. The support reactions within the elastic range of loading at a load 10 kN are listed in Table 1. for both straight and curved bridge models. The support reactions are expressed as percentage of the total applied load. For the straight bridge model the percentage of support reactions within the elastic range of loading was 28.0%, 20.2%, and 1.9%, respectively for the girder near load, the intermediate girder, and the girder far from load. Significant variation in the reaction distribution from a girder to another is observed. The ratio between the reaction of the girder far from load to that for the girder near load is about 1:15. Again, this is attributed to the fact that the load was eccentrically applied to the bridge model.

At failure, the percentage of support reactions for the straight bridge model was 21.3%, 16.67%, and 12.0%, respectively for the girder near load, the intermediate girder, and the girder far from load. It is observed that the distribution of support reactions at failure was much more uniform than that in the elastic range of loading. The ratio between the reaction of the girder far from load to that for the girder near load became about 1:1.8, compared to a ratio of 1:15 in the elastic range. This indicates a significant redistribution of support reactions at failure.

For the curved bridge model the percentage of support reactions within the elastic range at load 10 kN was 36.9%, 22.7%, and –9.6%, respectively for the girder near load, the intermediate girder, and the girder far from load. It should be noted that the negative sign of the support reaction of the girder far from load means an upward reaction indicating uplift. Comparing the results of the percentage of support reactions within the elastic range of loading for the straight bridge model to those for the curved bridge model, the effect of curvature can be detected. Such effect can be summarized as follows: (i) for the girder near load the percentage of support reaction increased from 28.0% for the straight

bridge model to 36.9% for the curved bridge model, representing about 32% increase as a result of curvature; (ii) for the intermediate girder the percentage of support reaction increased from 20.2% for the straight bridge model to 22.7% for the curved bridge model, representing about 12% increase as a result of curvature; and (iii) for the girder far from load the percentage of support reaction decreased from 1.9% for the straight bridge model to –9.6% for the curved bridge model indicating uplift.

From the above presented results it can be concluded that bridge curvature significantly influences the distribution of support reactions within the elastic range of loading in the following manner: (i) significant increase in the support reaction of the outer longer girder near load; (ii) increase in the support reaction for the intermediate girder; and (iii) significant decrease in the support reaction for the inner shorter girder far from load converting the downward reaction to an upward reaction indicating uplift. Furthermore, bridge curvature continued to influence the distribution of support reactions in the post-elastic range of loading up to failure as shown in fig. 9. It should be noted that in the post elastic range of loading the upward reaction of the girder far from load was reversed to a downward reaction due to the occurrence of the redistribution phenomena significantly.

At failure, for the curved bridge model the percentage of support reactions was 25.8%, 17.06%, and 7.18%, respectively for the girder near load, the intermediate girder, and the girder far from load. Comparing the results of the percentage of support reactions at failure for the straight bridge model to those for the curved bridge model, the effect of curvature may be summarized as follows: (i) for the girder near load the percentage of support reaction increased from 21.3% for the straight bridge model to 25.8% for the curved bridge model, representing about 21% increase as a result of curvature; (ii) for the intermediate girder the percentage of support reaction increased from 16.67% for the straight bridge model to 17.06% for the curved bridge model, representing about 2% increase as a result of curvature; and (iii) for the girder far from load the percentage of support reaction decreased from 12.0% for the straight bridge model to 7.18% for the curved bridge model, representing about 41% decrease as a result of curvature.

From the above presented results it can be concluded that bridge curvature influences the distribution of support reactions of reinforced concrete beam and slab bridges at failure. Such influence may be summarized as follows: (i) significant increase in the support reaction of the outer longer girder near load; (ii) increase in the support reaction of the intermediate girder; and (iii) significant decrease in the support reaction of the inner shorter girder far from load. Furthermore, the effect of bridge curvature on the distribution of support reactions was much more significant within the elastic range of loading than that at bridge failure. This is due to the fact that redistribution phenomena took place for both bridge models. However, redistribution was much more significant in the case of curved bridge model.

3.4. Cracking loads, failure loads, cracking patterns, and failure modes

Cracking loads and failure loads for the two tested beam-and-slab bridge models are listed in table 1. For the straight bridge model, the first crack appeared at a load 30 kN. The crack was vertical and formed at the vertical face of the girder near load. As the load was increased to 35 kN more vertical cracks were formed at the vertical face of the girder near load. At the same load a vertical crack was formed at the vertical face of the intermediate girder. At a load 40 kN more vertical cracks were formed at the vertical face of the girder near load and also of the intermediate girder. At this load a vertical crack was formed at the vertical face of the girder far from load. It should be noted that till a load 45 kN no cracks were observed at the bottom face of the slab. At this load 45 kN a transverse crack appeared at the bottom surface of the slab connecting the girder near load and the intermediate girder. At the same load transverse cracks were observed at the bottom face of the girder near load and the intermediate girder. As the load was increased cracks appeared at the bottom surface of the

slab connecting the intermediate girder and the girder far from load. Also, transverse cracks appeared at the bottom face of the girder far from load. Also, with increasing the load the following was observed: (i) increase in the length and width of all previously formed cracks; (ii) formation of more crack lines along the vertical and bottom faces of all longitudinal girders; and (iii) formation of more transverse crack lines at the bottom surface of the slabs connecting longitudinal girders. The cracks propagated until the bridge model failed at a load 70 kN. At failure, the following was observed: (i) formation of more crack lines for longitudinal girders and slabs; (ii) the strain in the longitudinal steel reinforcement exceeded the ultimate steel strain for both the girder near load and the intermediate girder; (iii) the bridge model failed when the longitudinal steel reinforcement in the girder far from load yielded; (iv) concrete crushing was observed on the upper surface of the bridge model; (v) a corner crack was formed at the top surface of the slab at the corners of the bridge model at the intersection of the girder far from load and the end diaphragm; and (vi) shear cracks appeared at the vertical faces of end diaphragms.

Similar observations were found for the curved bridge model in terms of the sequence of crack appearance and propagation. However, curvature significantly affected the values of the loads at which different cracks formed. For example, the first crack appeared in the case of curved bridge model was also vertical and also was formed at the vertical face of the longer outer girder near load. However, such crack was formed at a load 20 kN compared to a load of 30 kN in the case of straight bridge model which represents a 33.3% decrease in the cracking load as a result of curvature. The failure load was also significantly affected by bridge curvature. Such failure load was 50 kN for the curved bridge model compared to a load of 70 kN in the case of straight bridge model which represents about 29% decrease as a result of curvature. The mode of failure was not affected by bridge curvature. For both bridge models the failure mode was flexural by yielding of longitudinal/tangential steel reinforcement followed by concrete crushing. Fig. 10 shows cracking patterns for tested straight and curved beam-and-slab bridge models.

4. Theoretical study

An extensive theoretical study was conducted in this paper including a three-dimensional finite element modeling of curved reinforced concrete beam-and-slab bridges. A commercially available finite element package was used for the theoretical study. The reinforced concrete deck slab was modeled using a four-node shell element having six degrees of freedom at each node. The longitudinal girders, end diaphragms, and intermediate diaphragms were modeled using three-dimensional two-node beam elements with six degrees of freedom at each node. The finite element model is shown in fig. 11. The finite element model was used first to analyze the two reinforced concrete beam-and-slab bridge models tested in the current experimental program. Theoretical results for mid-span deflections and support reactions were compared to experimental ones. Good agreement was observed between the experimental results and the theoretical ones as shown in table 2. The difference between the experimental results and the theoretical ones for mid-span deflections did not exceed 7.6% except for the girder far from load in the case of curved bridge model. In this case the difference was 9.5%. Also, the theoretical results for support reactions showed a difference not exceeding 7.3% in comparison to the experimental ones.

4.1. Parametric study

The verified finite element model was then employed to conduct an extensive parametric study on prototype horizontally curved reinforced concrete beam-and-slab bridges. The parameters chosen for the study were: (i) degree of curvature of the bridge; (ii) longitudinal girder spacing; (iii) bridge aspect ratio; (iv) number of bridge traffic lanes; (v) number of longitudinal girders; (vi) number of intermediate diaphragms. Through the parametric study the following were assumed:

Fig. 11. Finite element model.

(i) all bridges considered were simply supported at both ends; (ii) all materials are elastic and homogeneous; and (iii) the effects of curbs are ignored. The number of traffic lanes considered was two, three, and four lanes, with bridge width of 8000 mm for two lane bridges, 12000 mm for three lane bridges, and 16000 mm for four lane bridges. The number of longitudinal girders ranged between three girders and eight girders. The span length at centerline considered ranged between 10000 mm and 30000 mm. The radius of curvature of the bridges ranged between 50000 mm and 150000 mm. The number of intermediate diaphragms considered ranged between three lines and six lines of diaphragms. It should be noted that all bridges considered in the parametric study were provided with end diaphragms.

More than 450 cases of curved reinforced concrete beam-and-slab bridges were considered in the parametric study. The standard truck specified in the Egyptian code for calculation of loads and forces in structures and buildings [28] was used through the parametric study. Such standard truck is shown in fig. 12. Many loading cases were considered in order to maximize the support reactions for different girders in the bridge. Trucks were also moved in the transverse direction within the loaded lanes in order to yield the maximum support reactions for bridge girders.

4.2. Results from the parametric study

For all prototype curved reinforced concrete beam-and-slab bridges considered in the parametric study the maximum reaction for a simply supported girder, R_s, under the effect of a line of wheel loads specified in the Egyptian code for calculation of loads and forces in structures and buildings [28], was first calculated for each girder. From the finite element analysis the maximum reaction R_{max} was obtained for each girder in all prototype bridges considered in the parametric study. Therefore, the reaction distribution factor D_r was calculated ($D_r = R_{max}/R_s$) for each girder in all prototype bridges. From the results of the parametric study it was found that the degree of curvature of the bridge is the most significant factor that affects the reaction distribution factor. Fig. 13 shows the relationship between the radius of curvature and the reaction distribution factor for a two-lane curved reinforced concrete beam-and-slab bridge having six longitudinal girders. Relationships are presented for the most outer girder, an intermediate girder, and the most inner girder. It can be observed that the reaction distribution factor decreases significantly, with increasing the radius of curvature, for both the most outer girder and the intermediate girder. However, for the most inner girder such factor increases significantly with increasing the radius of curvature of the bridge.

Fig. 12. Truck specified in the Egyptian code for the calculation of loads and forces in structures and buildings.

Fig. 13. Relationship between radius of curvature and reaction distribution factor.

Results, not presented herein for brevity, showed that the girder spacing is also one of the most important factors that affects the reaction distribution factor for all girders in curved reinforced concrete beam-and-slab bridges. Also, it was found that the number of intermediate diaphragms in the radial direction plays an important role in enhancing the distribution of support reactions in curved reinforced concrete beam-and-slab bridges. Increasing the number of intermediate diaphragms results in the following: (i) decrease in the reaction distribution factor for the most outer girder and the intermediate girders; and (ii) increase in the reaction distribution factor for the most inner girder.

4.3. Simplified empirical method for the calculation of support reactions in curved reinforced concrete beam-and-slab bridges

It was observed from the results of the parametric study that the most significant factors that affect the reaction distribution factors in curved reinforced concrete beam-and-slab bridges are: degree of curvature of the bridge, longitudinal girder spacing, and number of intermediate diaphragms in the radial direction. Using a commercially available statistical package for best fit, the data generated from the parametric study including more than 450 cases of curved reinforced concrete beam-and-slab bridges was employed to develop simple empirical formulas for the calculation of the reaction distribution factors for different girders in the bridge. The empirical formulas developed in this paper are in terms of the following parameters: (i) radius of curvature of the bridge, R_c, in meters; (ii) longitudinal girder spacing expressed as the dimensionless parameter, S_g = number of traffic lanes/number of longitudinal girders; and (iii) number of intermediate diaphragms in the radial direction, N_d. Therefore, the empirical formulas developed in this paper can be presented as follows:

- *For the most outer girder:*

$$D_r = 1.52 - 0.0034\,R_c + 1.25\,S_g - 0.14\,N_d. \quad (1)$$

- *For the intermediate girder:*

$$D_r = 1.61 - 0.0047\,R_c + 1.99\,S_g - 0.091\,N_d. \quad (2)$$

- *For the most inner girder:*

$$D_r = -0.56 + 0.0029\,R_c + 1.23\,S_g + 0.094\,N_d. \quad (3)$$

4.4. Illustrative example

It is required to calculate the maximum support reactions for different girders in a two-lane curved reinforced concrete beam-and-slab bridge having five longitudinal girders. The bridge details are as follows: span length of the bridge at centerline = 30.0 meters; total bridge width = 8.0 meters; central angle of the bridge = 17.2 degrees; radius of curvature of the bridge at centerline = 100.0 meters; longitudinal girder spacing = 2.0 meters; and number of intermediate diaphragms in the radial direction = 5. Solution: the dimensionless parameter S_g = number of traffic lanes/number of longitudinal girders = 2/5 = 0.4. Applying a line of wheel loads of the standard truck specified in the Egyptian code for calculation of loads and forces in structures and buildings [28] on a simply supported girder the reaction R_s for the most outer girder is 285.6 kN, for an intermediate girder is 285.0 kN, and for the most inner girder is 284.4 kN. The reaction distribution factor, D_r, for the most outer girder using eq. (1) is 0.98, therefore R_{max} = 0.98 × 285.6 = 279.89 kN. The reaction distribution factor, D_r, for the intermediate girder using eq. (2) is 1.48, therefore R_{max} = 1.48 × 285.0 = 421.8 kN. The reaction distribution factor, D_r, for the most inner girder using eq. (3) is 0.69, therefore R_{max} = 0.69 × 284.4 = 196.2 kN.

5. Summary and conclusions

Detailed literature review was conducted including all available previous investigations in the behavior of reinforced concrete beam-and-slab bridges. It was observed that most of the investigations found have been directed towards rectangular straight bridges. Comparatively, very little research efforts have

considered the behavior of horizontally curved reinforced concrete beam-and-slab bridges. None of the previous investigations found in the literature has considered the behavior of horizontally curved reinforced concrete beam-and-slab bridges in the post elastic range of loading up to failure. None of the previous investigations found in the literature has considered the distribution of reactions in horizontally curved reinforced concrete beam-and-slab bridges over the complete range of loading up to failure. An experimental program was conducted in this paper included the fabrication, instrumentation, and testing of two reinforced concrete beam-and-slab bridge models. One of these bridge models was rectangular in plan whereas the other bridge model was horizontally curved. Thus the effect of curvature was extensively investigated when comparing the results of testing the two bridge models. A finite element model was developed. The reliability of the model was confirmed using the current experimental results. The finite element model was then employed to conduct a detailed parametric study on prototype horizontally curved reinforced concrete beam-and-slab bridges. The effect of all major parameters on the support reactions was investigated. Finally the results of the parametric study was used to develop a simple empirical method for the calculation of support reactions in horizontally curved reinforced concrete beam-and-slab bridges utilizing the standard truck specified in the Egyptian code for calculation of loads and forces in structures and buildings [28]. Based on this study the following conclusions were drawn.

1. Bridge curvature significantly influences the deflection and steel strains of the longitudinal girders of reinforced concrete beam and slab bridges within the elastic range of loading in the following manner: (i) significant increase in the deflection and steel strain of the outer longer girder; and (ii) significant decrease in the deflection and steel strain of the inner shorter girder.
2. Bridge curvature continued to influence longitudinal girders deflection and steel strain of reinforced concrete beam-and-slab bridges in the post-elastic range of loading up to failure. Bridge curvature influences the deflection and steel strain of the longitudinal girders of reinforced concrete beam and slab bridges at failure in the following manner: (i) increase in the deflection and steel strain of the outer longer girder; (ii) increase in the deflection and steel strain of the intermediate girder; and (iii) decrease in the deflection and steel strain of the inner shorter girder.
3. The effect of bridge curvature on the deflection and steel strain of the longitudinal girders of reinforced concrete beam-and-slab bridges is much more significant within the elastic range of loading than that at failure. Such variation in the effect of bridge curvature may be attributed to the fact that in the case of curved bridges redistribution phenomena have significantly took place at failure leading to a more uniform distribution of loads between longitudinal girders.
4. Bridge curvature significantly influences the distribution of support reactions within the elastic range of loading in the following manner: (i) significant increase in the support reaction of the outer longer girder near load; (ii) increase in the support reaction for the intermediate girder; and (iii) significant decrease in the support reaction for the inner shorter girder far from load converting the downward reaction to an upward reaction indicating uplift.
5. Bridge curvature continued to influence the distribution of support reactions in the post-elastic range of loading up to failure. In the post elastic range of loading the upward reaction of the girder far from load was reversed to a downward reaction due to the occurrence of the redistribution phenomena significantly. Furthermore, the effect of bridge curvature on the distribution of support reactions was much more significant within the elastic range of loading than that at bridge failure. This is due to the fact that redistribution phenomena took place for both bridge models. However, redistribution was much more significant in the case of curved bridge model.
6. The sequence of crack appearance and propagation was not affected by bridge curvature. However, curvature significantly affected the values of the loads at which different cracks formed. Also, cracking load

decreased significantly as a result of bridge curvature.
7. The bridge failure load was significantly affected by bridge curvature. Such failure load decreased as a result of curvature. The mode of failure was not affected by bridge curvature. For both bridge models the failure mode was flexural by yielding of longitudinal/tangential steel reinforcement followed by concrete crushing.
8. Based on the theoretical study conducted on this paper using the finite element method analyzing prototype curved reinforced concrete beam-and-slab bridges under the standard truck specified in the Egyptian code, it was found that the most important parameters that affect the reaction distribution in such type of bridges are degree of curvature, girder spacing, and number of intermediate diaphragms in the radial direction.

Acknowledgments

The test program in this paper was carried out during 2005 at the Reinforced Concrete Research Laboratory, Alexandria University. The author would like to thank all the technicians of the laboratory for their helpful assistance in the preparation and testing the bridge models.

References

[1] R. Nagaraja, and S.D. Lash, "Ultimate Load Capacity of Reinforced Concrete Beam-and-Slab Highway Bridges", ACI Structural Journal, Vol. 67 (12), pp. 1003-1009 (1970).
[2] T.J. Lbell, C.T. Morley and C.R. Middleton, "Strength and Behavior in Shear of Concrete Beam-and-Slab Bridges", ACI Structural Journal, Vol. 96 (3), pp. 386-391 (1999).
[3] A.K. Azad, M.H. Baluch, M.S.A. Abbasi and K. Kareem, "Punching Capacity of Deck Slabs in Girder-Slab Bridges", ACI Structural Journal, Vol. 91 (6), pp. 656-662 (1994).
[4] A.A. Mufti and J.P. Newhook, "Punching Shear Strength of Restrained Concrete Bridge Deck Slabs", ACI Structural Journal, Vol. 95 (4), pp. 375-381 (1998).
[5] L. Deng, M. Ghosn, A. Znidaric and J.R. Casas, "Nonlinear Flexural Behavior of Concrete Girder Bridges", ASCE Journal of Bridge Engineering, Vol. 6 (4), pp. 276-284 (2001).
[6] M. Schwarz and J.A. Laman, "Response of Concrete I-Girder Bridges to Live Load", ASCE Journal of Bridge Engineering, Vol. 6 (1), pp. 1-18 (2001).
[7] L. Cao, J.H. Allen, P.B. Shing and D. Woodham, "Behavior of RC Bridge Decks with Flexible Girders", ASCE Journal of Structural Engineering, Vol. 122 (1), pp. 11-19 (1996).
[8] M.I. Soliman, A.S. Abdel-Faiad, O.H. Abdel-Wahed and K.E.M. Mohamed, "Response of Continuous Haunched R.C. Girder Type Bridges with and Without Bottom Slab Under Coupled Vertical Loads", Proceedings of the Eighth International Colloquium on Structural and Geotechnical Engineering, Ain Shams University, Cairo, Egypt, pp. 1-16 (1998).
[9] M.M.A. El-Metwally, "Behavior of Simple and Continuous Bridges Under Codes Truck Axle Loading", Proceedings of the Fourth International Colloquium on Structural and Geotechnical Engineering, Alexandria University, Alexandria, Egypt, pp. 411-417 (2001).
[10] American Association of State Highway and Transportation Officials (AASHTO), "AASHTO Bridge Design Specifications, 2nd Edition", Washington, D.C., U.S.A. (1998).
[11] K.M. Tarhini and G.R. Frederick, "Lateral Load Distribution in I-Girder Bridges", Journal of Computers and Structures, Vol. 54 (2), pp. 351-354 (1995).
[12] S. Kim and A.S. Nowak, "Load Distribution and Impact Factors for I-Girder Bridges" ASCE Journal of Bridge Engineering, Vol. 2 (3), pp. 97-104 (1997).
[13] C.H. Liu, T.L. Wang and M. Shahawy, "Load Lateral Distribution For Multigirder Bridges", Proceedings of the First MIT Conference on Computational Fluid and Solid Mechanics, Massachusetts Institute of Technology,

Cambridge, Massachusetts, U.S.A. (2001).

[14] M. Shahawy and D. Huang, "Analytical and Field Investigation of Lateral Load Distribution in Concrete Slab-on-Girder Bridges", ACI Structural Journal, Vol. 98 (4), pp. 590-599 (2001).

[15] P.J. Barr, M.O. Eberhard and J.F. Stanton, "Live Load Distribution Factors in Prestressed Concrete Girder Bridges", ASCE Journal of Bridge Engineering, Vol. 6 (5), pp. 298-306 (2001).

[16] M. Mabsout, K. Tarhini, R. Jabakhanji and E. Awwad, "Wheel Load Distribution in Simply Supported Concrete Slab Bridges", ASCE Journal of Bridge Engineering, Vol. 9 (2), pp. 147-155 (2004).

[17] D.H. Tobias, R.E. Anderson, S.Y. Khayyat, Z.B. Uzman and K.L. Riechers, "Simplified AASHTO Load and Resistance Factor Design Girder Live Load Distribution in Illinois", ASCE Journal of Bridge Engineering, Vol. 9 (6), pp. 606-613 (2004).

[18] M. Saiidi, J.D. Hart and B.M. Douglas, "A Nonlinear Model for Static and Dynamic Transverse Load Analysis of Reinforced Concrete Highway Bridges", Journal of Computers and Structures, Vol. 26 (5), pp. 831-840 (1987).

[19] M.A. Crisfield, "Numerical Methods for the Non-Linear Analysis of Bridges" Journal of Computers and Structures, Vol. 30 (3), pp. 637-644 (1988).

[20] A.S. Nowak and M.M. Szerszen, "Bridge Load and Resistance Models", Journal of Engineering Structures, Vol. 20 (11), pp. 985-990 (1998).

[21] H.W. Song, D.W. You, K.J. Byun and K. Maekawa, "Finite Element Failure Analysis of Reinforced Concrete T-Girder Bridges", Journal of Engineering Structures, Vol. 24 (2), pp. 151-162 (2002).

[22] J.S. Davidson, R.S. Abdalla and M. Madhavan, "Design and Construction of Modern Curved Bridges", Department of Civil and Environmental Engineering, The University of Alabama at Birmingham, Birmingham, Alabama, U. S. A., pp. 18 (2002).

[23] A. Aly and J.B. Kennedy, "Curved Structures in Waffle Slab Construction", Journal of Engineering Structures, Vol. 16 (8), pp. 591-601 (1994).

[24] A. Aly, and J.B. Kennedy, "Design of Horizontally Curved Waffle Slab Structures", Journal of Engineering Structures, Vol. 19 (1), pp. 37-49 (1997).

[25] Y.L. Pi and N.S. Trahair, "Nonlinear Elastic Behavior of I-Beams Curved in Plan", ASCE Journal of Structural Engineering, Vol. 123 (9), pp. 1201-1209 (1997).

[26] W. Kim, Live Load Moment Distribution for Horizontally Curved I-Girder Bridges, Master of Science Thesis, the Pennsylvania State University, University Park, PA (2004).

[27] American Association of State Highway and Transportation Officials (AASHTO), "Guide Specifications for Horizontally Curved Highway Bridges", Washington D.C., U. S. A. (1993).

[28] Housing and Building Research Center, Ministry of Housing and Utilities, "Egyptian Code for Calculation of Loads and Forces in Structures and Buildings", Cairo, Egypt, pp. 76 (1993).

Received July 24, 2006
Accepted September 25, 2006